https://doi.org/10.2352/EI.2022.34.16.AVM-214

Original Image Noise Reconstruction for Spatially-Varying Filtered Driving Scenes

Luis Constantin Wohlers[1] , Patrick Müller[1] , Alexander Braun[1] ;
[1]University of Applied Sciences Düsseldorf; Düsseldorf, Germany

Abstract

Test drives for the development of camera-based automotive algorithms like object detection or instance segmentation are very expensive and time-consuming. Therefore, the re-use of existing databases like COCO or Berkeley Deep Drive by intentionally varying the image quality in a post-processing step promises to save time and money, while giving access to novel image quality properties. One possible variation we investigate is the sharpness of the camera system, by applying spatially varying optical blur models as low-pass filters on the image data. Any such operation significantly changes the amount and distribution of noise, a central property of image quality, which in this context is an undesired side-effect. In this article, a novel method is presented to reconstruct the original camera sensor noise for the filtered image. This is different from denoising. The method estimates the original camera sensor noise using the combination of principal component analysis (PCA) and a variance-stabilizing transformation. The noise is then reconstructed for the filtered image with the PCA applied locally on small image sections, and an inverse variance-stabilizing transformation. Although the resulting noise distribution can slightly deviate from the original, this novel method does not introduce any image artifacts as denoising would do. We present the method as applied to synthetic and real driving scenes at different noise levels and discuss the accuracy of the reconstruction visually and with statistical parameters.

Introduction

Noise is an important characteristic of image quality in general, and for camera-based advanced driver assistance systems (ADAS) and autonomous driving (AD) in particular. Noise has many established metrics associated with it, like signal-to-noise-ratio (SNR) and Peak-SNR (PSNR) or dark-signal non-uniformity (DSNU), and current novel proposals like Contrast Detection Probability (CDP)[4, 2] or Sensitivity (SNRi)[10]. The EMVA 1288 standard[24] is a well-known and well-used process to characterize image sensor noise properties, and the IEEE P2020 working group on automotive image quality is extending this foundation for the special needs of the automotive industry[7].

Noise has a distinct influence on the downstream evaluation algorithms working on images. In the context of ADAS/AD these algorithms for detection and planning are predominantly based on machine learning (ML) and artificial neural networks (ANN), and as such sensitive in general to this influence[21, 3]. In real camera systems there is an important distinction between the two use-cases of human perception and computer vision, and this directly relates to the influence the noise has. Humans prefer images free of noise and with sharp edges, whereas computer vision algorithms prefer the opposite, i.e. a normal texture appearance including noise and edges that are left untreated. This use-case dependency is reflected in the configuration of the image signal processor (ISP), a central preprocessing component used in every current ADAS system. A typical ISP performs amongst others gain and color correction, and of course denoising and sharpening, before handing this processed image data to the actual evaluation algorithm.

Our research focuses on the influence optical and imaging properties have on typical ML-based computer vision tasks, like object detection or recognition, or semantic and instance segmentation. We have developed novel degradation models that transform a given image as if recorded by a different lens with different optical properties.[15, 14, 17, 13] This lens is applied like a filtering process on a given image database, and thus allows for the parameterized simulation of different optical properties.

This work examines the influence of our optical models on the noise present in prerecorded scenes. As a filtering operation the optical model will always be a low-pass filter, decreasing and correlating the noise present in the images. Therefore, we present a novel method to reconstruct the original noise. First, we quantitatively determine the amount of noise present, then compare the noise before and after the optical filtering, in order to determine the difference between the two. Finally, the amount of missing noise can be added back to the filtered image, giving a blurred image with the correct amount of noise, as a real camera would. This process then allows for the re-use of existing drive scene databases, by first applying the optical model and then reconstructing the noise, such that the robustness of the evaluation algorithm with regard to the optical changes can be quantified.

One aspect of this work is particularly worth highlighting: all operations are *spatially variable*. I.e. both the optical blurring varies over field, and the noise is scene dependent as well, and thus varies over field. We take both variations into account, and this – beside the actual use-case – is the main novelty presented in this paper.

The Noise Model

As the main topic of this work is the reconstruction of noise parameters in filtered images, it is critical to define a noise model that realistically represents image sensor noise. In the context of automotive cameras, specifically CCD (charge-coupled devices) and CMOS (complementary metal-oxide-semiconductor) sensors are of interest. The signal-dependent noise model is introduced in this section. As a means to transform signal-dependent noise into signal-independent noise, a variance-stabilizing transformation is introduced.

The Signal-Dependent Linear Model

In this work, a signal-dependent noise model is assumed, which is similar to the well-known EMVA 1288 standard for camera characterisation [24]. The model is used in Pytaykh's work [23] as well as in [8]. The noise model is valid for both CCD and CMOS sensors as the underlying physical pixel model of a number of electrons being generated through absorption of photons and then converted into a digital gray value is the same regardless of sensor technology [8, 24]. As the exact irradiation conditions in the task at hand are unknown, the noise model considered here is the same for all pixels. Physical properties such as the system gain or the quantum efficiency [24] are abstracted into noise parameters a and b [23]. Two main noise sources are considered: Noise stemming from temperature induced electrons, readout noise and other hardware effects as "dark noise" which is present even without any irradiation as well as photon shot noise. [9] The dark noise is assumed to be approximately normally distributed with mean zero. If $\xi(\mathbf{p})$ is considered a random variable $\xi(\mathbf{p}) \sim \mathcal{N}(0,1)$ with $\mathbf{p} \in \mathbb{Z}^2$ being a pixel location, then the dark signal can thus be expressed as $\sqrt{b}\xi(\mathbf{p}) \sim \mathcal{N}(0,b)$ [23]. The dark noise is expressed as a function of the location, but the variance of the dark signal itself does not depend on the pixel location. The number of photons incident on the pixel surface however depends on the pixel location, as the accumulation of photons during exposure is a counting process following a Poisson distribution depending on a pixel's irradiation [24]. Considering now a Poisson-distributed random variable $\omega(\mathbf{p}) \sim \mathcal{P}(\mu_p(\mathbf{p}))$ [23], where $\mu_p(\mathbf{p})$ is the mean number of photons incident on a pixel, an image $y = y(\mathbf{p})$ can be expressed as

$$y(\mathbf{p}) = a\omega(\mathbf{p}) + \sqrt{b}\xi(\mathbf{p}) \tag{1}$$

[23], where a is a parameter depending on the sensor's quantum efficiency and system gain [9]. The image $y = y(\mathbf{p})$ can be related to the noise free image $x(\mathbf{p})$. If further $\omega(\mathbf{p})$ is replaced with the normal-distributed $\omega_N(\mathbf{p})$, equation 1 can be expressed as

$$y(\mathbf{p}) = a\omega_N(\mathbf{p}) + \sqrt{b}\xi(\mathbf{p}) = x(\mathbf{p}) + \sqrt{ax(\mathbf{p})+b}\xi(\mathbf{p}) \tag{2}$$

[23]. In this expression, the noise does not consist of a mix of signal-dependent Poisson and signal-independent Gaussian noise as in equation 1, but only of signal-dependent Gaussian noise.

Variance Stabilizing Transformation

In image processing, variance stabilizing transformation is a non-linear gray value transformation that is applied in order to equalize $y(\mathbf{p}) = x(\mathbf{p}) + \sqrt{ax(\mathbf{p})+b}\xi(\mathbf{p})$ has to be transformed into

$$y_S(\mathbf{p}) = x_S(\mathbf{p}) + \sqrt{\sigma_S^2}\xi(\mathbf{p}), \tag{3}$$

where $x_S(\mathbf{p})$ is the transformed noise-free image and σ_S^2 is the stabilized variance which is signal-independent. Variance stabilizing transformation is a non-linear function of a random variable obtained by approximating the variance using a first order Taylor series around the mean vector.[8] Further, setting the variance to a constant value and subsequently integrating yields the variance stabilizing transformation of $y(\mathbf{p})$ with parameters a and b:

$$y_S(\mathbf{p}) = f(y(\mathbf{p}); a, b) = \frac{2\sigma}{a}\sqrt{ay(\mathbf{p})+b} \tag{4}$$

[23]. The noise in the resulting image $y_S(\mathbf{p})$ is now approximately normally distributed with signal-independent variance σ.

As the approximation of a non-linear equation requires sufficiently linear behaviour around the mean [8], the VST is less accurate when the non-linear component of the approximated equation is large. Considering modern image sensors, we assume the parameter a to be well within the range $a \leq 20$ for which Pyatykh [23] has shown the variance stabilizing transformation in equation 4 to be accurate.

PCA for Noise Parameter Estimation

Principal component analysis (PCA) is a method for data dimensionality reduction. It was first introduced by Karl Pearson [20] and later described and named by Harold Hotelling [6]. PCA and variants are used in a variety of applications, such as image compression [1], or denoising and pattern recognition [12, 5]. For accurate estimation of image noise parameters of a signal dependent noise model, PCA is combined with variance stabilizing transformation and "normality assessment" [23, 22]. In the context of this work, it is used for noise parameter estimation and the method to reconstruct the noise parameters in a filtered image is also derived from Pyatykh's method. PCA and its applications are well described in literature such as in [6, 11, 22, 23].

The noise variance estimation method by application of PCA as described by Pyatykh [22] can be summarized for images corrupted with normally distributed signal-independent noise as follows: A noise-free image, represented as a signal $x(\mathbf{p})$, where $\mathbf{p} \in \mathbb{Z}^2$ is the pixel location, is considered to be unknown and corrupted with normally distributed noise, represented as a noise signal $n(\mathbf{p})$ whose elements are normally distributed random variables $n(\mathbf{p}) \sim \mathcal{N}(0,\sigma^2)$ with mean 0 and variance σ^2. The noisy image is then given by $y(\mathbf{p}) = x(\mathbf{p}) + n(\mathbf{p})$. The signal notation for these images is equivalent to a matrix representation.

Extraction of a dataset $\mathbf{Y} = [\mathbf{y}_1\ \mathbf{y}_2\ \ldots\ \mathbf{y}_n]$ from such an image is performed by sliding a rectangular binary pixel mask $\mathbf{M}$ of dimensions $B' \times B'$ over the image, extracting the underlying pixel values, arranging them in a vector and repeating the step to yield n column-vectors of size $p \times 1$ arranged in $\mathbf{Y}$. It is assumed that the underlying unknown noise free image could be represented in less than p dimensions if sampled in the same way. The latent variables $\lambda_1, ..., \lambda_p$ are thus computed, where $\lambda_p = \sigma^2$. [22] The challenge in application of Pyatykh's method is mostly to find a good number p of principal components to compute, which has to be large enough to warrant that λ_p is not influenced by image content anymore and small enough to be able to extract a large number of vectors from the image in order to obtain a reliable dataset. These challenges are addressed as well in [22].

Note that PCA as described before is also only applicable for signals which are corrupted with signal-independent noise. In order to apply the technique to estimate the noise parameters a and b of the approximated noise model

$$y(\mathbf{p}) = x(\mathbf{p}) + \sqrt{ax(\mathbf{p})+b}\xi(\mathbf{p}), \tag{5}$$

the technique is combined with a variance stabilizing transformation as described in [23]. The method mainly consists of optimizing parameters a and b such that the noise in the transformed image

$$y_S(\mathbf{p}) = \frac{2\sigma}{a}\sqrt{ay(\mathbf{p})+b} \tag{6}$$

is signal-independent normally distributed noise with variance σ. An iterative optimization process is used where in each step a new set of estimated parameters is used to transform the original image, the noise in this image is analysed and the normality of the noise distribution is tested using Mardia's test for multivariate normality [16].

Optical model and filtering

An optical system can be characterised by its intensity point spread function (PSF), which describes the spread of a point source after propagation through the optical system. The PSF describes effects such as diffraction phenomena and lens aberrations and is considered a non-linear and space-variant function.[19, 15, 14]. Often the space-variance is neglected, if it can be assured that details of the introduced blur don't matter. However, in the context of physical-realistic models, the local PSF varies across the imager. In this case, different methods exist to apply the PSFs on images.[19] In this article, we demonstrate the noise reconstruction method on images degraded with the space-variant blur model from [18]. The filtered images then mimic an image taken with a Cooke triplet, which produces lens aberrations such as astigmatism and chromatic aberration. As with real lenses, these aberrations can vary across the image, unlike spatially invariant models.

Influence of Filtering Operations on the Noise Distribution

Generally speaking, any filtering operation transforms "white" noise, in which the spectral density of the noise is independent of the frequency, into "coloured" noise whose spectral density depends on the frequency. For example, a low pass applied to a noisy signal will not only influence the signal itself but also the noise, whose high frequency components will be suppressed. Speaking in terms of statistical noise analysis, this means that uncorrelated noise is transformed into correlated noise. Concerning the noise model given before, a filtered image still has some parameters a and b, but the random variable $\xi(\mathbf{p})$ is influenced in a way that after filtering the noise variables of adjacent pixels are not uncorrelated to each other anymore. Depending on the particular filter, the noise of all pixels in a specific image region is correlated. If a real optical system's PSF is regarded as having similar low-pass characteristics to a gaussian filtering operation [15, 13], then the variance of the noise in the filtered image is lower than that in the original image. However, the noise distribution in a filtered image is only easy to describe mathematically as long as the filtering operation is space-invariant, the filter mask is symmetric and the noise is signal-independent, making a precise analysis of the actual noise parameters in a filtered image almost infeasible.

Noise Reconstruction on Filtered Images

Our method for noise reconstruction on filtered images is based on the principle of adding noise back to the filtered image such that the overall noise variance in the resulting image is the same as the noise variance in the original image. This concept is visualized in figure 1. Figure 1a shows normally distributed uncorrelated noise. The same noise distribution is shown in figure 1b after applying a Gaussian low-pass filter. The characteristic, smoother appearance of correlated noise can clearly be noted. Comparing the histograms of the unfiltered (1d) and filtered distribution (1e), the effect of low-pass filtering on the variance already described in the previous section is obvious. 1c and 1f are then obtained by adding normally distributed noise back on to the filtered distribution such that is has the same variance as the unfiltered distribution, seen in the histogram in 1f. Regarding the visual result of this reconstruction step, 1c displays strong similarity to 1a. Our method can therefore be built around the basic principle of simply adding noise under the assumption that the effect of low-pass filtering on image noise is strong enough such that the influence of the filtered noise on the visual result of the reconstructed image is low. The quality of reconstruction then depends on the variance of the correlated noise after filtering. Figure 2 serves to explain the

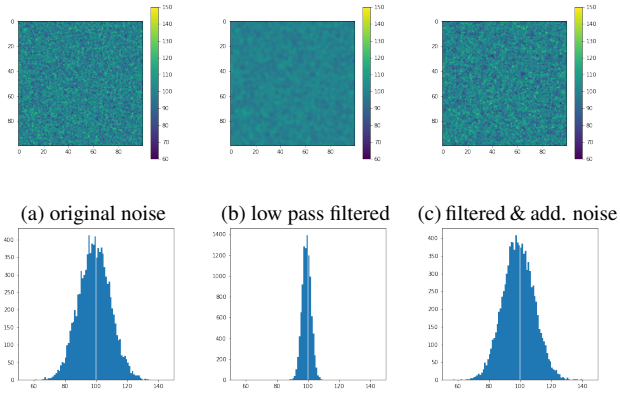

(a) original noise (b) low pass filtered (c) filtered & add. noise

(d) histogram of original noise (e) histogram of filtered noise (f) histogram of reconstructed noise

Figure 1: Simple illustration of the image signal path: A noisy image is filtered using a Gaussian filter and noise reconstruction is performed by adding noise back onto the filtered image.

use of variance stabilizing transformation for noise reconstruction in this context on a one-dimensional signal: Subfigure 2a presents a noisy signal with some noise parameter θ describing signal-dependent noise, visible in the different variance at lower and higher signal amplitudes. Figure 2b then demonstrates the variance stabilized original signal. Time-variant filtering of the original signal is simulated in figure 2c by applying three low-pass filters with different strength on three signal parts. On this filtered signal, a VST with respect to the original noise parameter θ is applied, the result of this is shown in figure 2d. On first sight, the use of this step is not obvious. However, noise reconstruction can now be performed by adding noise in such a way that this signal presents a valid variance stabilized version of the desired final signal: This is illustrated in figure 2e, where noise has been added such that we now have the same signal-independent variance in all signal segments. The final signal with reconstructed noise of the desired signal-dependent behaviour is then obtained by applying the inverse of the VST with respect to θ. While a one-dimensional signal serves well to demonstrate the general idea, this method can be applied to images, i.e. two-dimensional signals, as well. In order to use this basic framework of the presented method, some requirements have to be fulfilled: The original image as well as the corresponding noise model has to be known

such that the original noise parameters can be estimated. Additionally, the existence of a variance stabilizing transformation corresponding to the noise model is crucial. With regards to the application considered in this work, the original image is always available and the noise model as well as the corresponding VST has already been described. To estimate the original noise parameters, we use Pyatykh's noise parameter estimation method. It now remains to describe how the task of determining the correct amount of noise to add back onto each image pixel to equalize the noise variance in the reconstruction step (represented by figure 2e in our one-dimensional example) can be tackled.

Estimation of local noise variance in a spatially varying filtered and transformed image is done by local application of PCA. This means that the basic notion of Pyatykh's noise variance estimation method [22], extracting a dataset and computing the variance explained by the smallest principal component, is performed on small image regions. These image regions are chosen such that each pixel of an $M \times N$ image is at the center of one region of size $W \times W$, requiring some form of padding at the image edges. In figure 3, this concept is illustrated. To ensure approximate noise variance estimation at the image edges, we choose symmetric padding. The padded image is then of size $(M+2w') \times (N+2w')$ with $w' = \lfloor W/2 \rfloor$. As described in the section "PCA for Noise Parameter Estimation", a dataset is then extracted using a sliding window of size $B \times B$ and PCA is performed to estimate the noise variance. The result is assumed to approximately represent the remaining noise variance on the image window's central pixel. The difference between this value σ^2_{PCA} and the desired variance σ_{VST} used for the VST is computed and a sample from a normally distributed random variable $X \sim \mathcal{N}(0, \sigma^2)$, where $\sigma = \sqrt{\sigma^2_{VST} - \sigma^2_{PCA}}$, is added to the pixel's grey value in a copy of the filtered and transformed image in question. This procedure is repeated for every pixel, such that the $W \times W$ image window can be regarded as a sliding window over the complete image area. It is crucial to write the final pixel grey values into a copy of the image as to not skew the variance estimation process. This copy is finally transformed into the desired image with reconstructed signal-dependent noise by the corresponding inverse VST, which in the case of the noise model considered in this work is

$$y_{rec}(\mathbf{p}) = \frac{a y^2_S(\mathbf{p})}{4\sigma^2_{VST}} - \frac{b}{a}. \tag{7}$$

In algorithm 1, the complete procedure is presented as a function taking the estimated noise parameters as well as the dimensions W and B as inputs. For rgb images, this algorithm has to be performed separately on each color channel.

Our method is applicable under the assumption that the image section size W can be chosen to be small enough such that the variance computed by PCA is representative of the central pixel's actual noise despite the strongly space variant filtering and the subsequent transformation with respect to the original noise parameters. As a smaller image window and thus smaller dataset size necessarily results in a higher variance of the noise estimation, underestimation of the actual noise variance at smaller window sizes W may be balanced out by this effect. We find $W = 9$ and $B = 3$ to be the smallest parameters yielding good results, resulting in a dataset of size 49×9 at each segment and 9 principal components computed by PCA.

Algorithm 1: Noise Reconstruction

function ReconstructNoise $(\mathbf{y}_f, a, b, W, B)$;
Input : Filtered version $\mathbf{y}_f$ of $M \times N$ image $\mathbf{y}$, noise parameters of original image $\mathbf{y}$ a and b, window size W, block size B
Output: Reconstructed image $\mathbf{y}_{rec}$
$\mathbf{y}_{f,vst} \leftarrow VST(\mathbf{y}_f, a, b, \sigma_{VST} = 1)$
pad image $\mathbf{y}_{f,vst}$
for $m = 0, 1, ..., M-1$ **do**
  for $n = 0, 1, ..., N-1$ **do**
    $Y \leftarrow$ extract image window of size $W \times W$ around pixel $\mathbf{y}_{f,vst}[m][n]$
    $D \leftarrow$ extract $(W-B+1)^2 \times B^2$ dataset from Y using a sliding window of size $B \times B$
    $\sigma^2_{PCA} \leftarrow$ compute value $\lambda_{B^2}(D)$ by PCA on D as an estimate of the variance of remaining uncorrelated noise
    $\sigma \leftarrow \sqrt{\sigma^2_{VST} - \sigma^2_{PCA}}$
    $\mathbf{y}_{rec,vst}[m][n] \leftarrow \mathbf{y}_{f,vst}[m][n] + sample(\mathcal{N}(0, \sigma^2))$
  end
end
return $\mathbf{y}_{rec} \leftarrow inverseVST(\mathbf{y}_{rec,vst}, a, b, \sigma_{VST})$

orig. a	rec. a	orig. b	rec. b
0.96	0.91	54.57	57.52
1.03	1.01	47.63	47.34
1.05	1.08	46.81	43.02
1.0	0.96	50.56	53.07
1.02	0.99	49.15	48.51
0.85	0.84	60.11	59.47

Table 1: Example results from the red channel of six images with noise parameters $a \approx 1$ and $b \approx 50$

Results

In this section, we present results from application of our method on noisy images degraded with an optical model, focusing on showing the correct reconstruction of the original noise parameters as well as the space-variant behavior of the method. We also briefly point out the influence of noise reconstruction on PSNR. Finally, as an exemplary demonstration of the effect on computer vision algorithms, we degrade and reconstruct a number of images and observe the influence these operations have on the performance of a detection algorithm.

Noise parameter reconstruction

In table 1, the noise parameters of the red channel of six images from the BDD100k dataset [25] corrupted with synthetic noise with parameters $a \approx 1$ and $b \approx 50$ are presented before degradation (columns "orig. a" and "orig. b") as well as after degradation and subsequent application of our noise reconstruction technique (columns "rec. a" and "rec. b"). In order to evaluate the method without any unwanted effects of quantization at very low noise levels, we chose to add synthetic noise according to the considered noise model to real images with negligibly low noise. Noise parameters are additionally estimated before applying our method as to simulate the whole process and point out the influence of the parameter estimation method in use on the

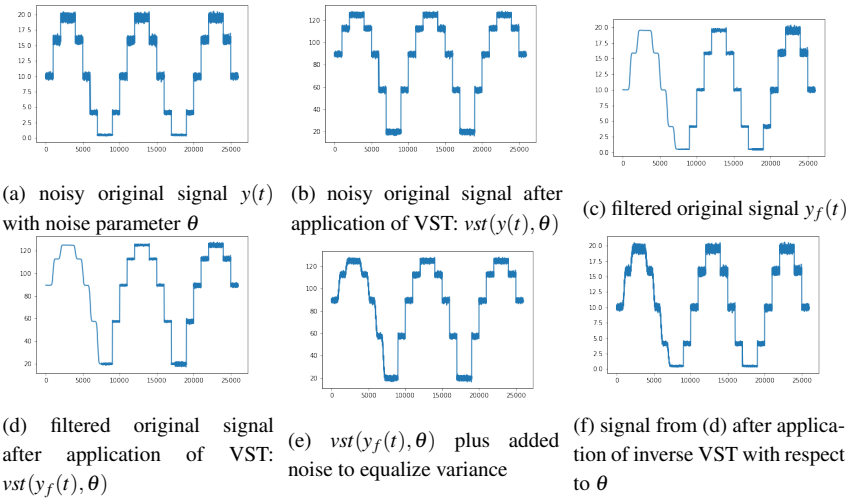

(a) noisy original signal $y(t)$ with noise parameter θ

(b) noisy original signal after application of VST: $vst(y(t),\theta)$

(c) filtered original signal $y_f(t)$

(d) filtered original signal after application of VST: $vst(y_f(t),\theta)$

(e) $vst(y_f(t),\theta)$ plus added noise to equalize variance

(f) signal from (d) after application of inverse VST with respect to θ

Figure 2: process of filtering and noise reconstruction shown on a 1d signal

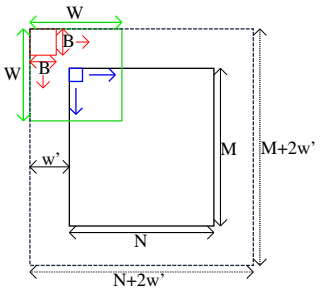

Figure 3: noise reconstruction method dimensions

Figure 4: Image from BDD100k with added noise and degraded by an optical model, with ROIs from figures 5 (red) and 6 (green)

method's applicability. Estimation of the parameters of the reconstructed method are performed using Pyatykh's method as well and with the same hyperparameters. Comparing the values of reconstructed and original parameters, our method achieves sufficient accuracy. It has to be noted, however, that the outcome also depends strongly on the accuracy of the noise parameter estimation method in use at the respective noise parameters.

The space variant behavior of our method is shown in figure 5, where a section of an image from the BDD dataset corrupted with strong synthetic noise is presented before filtering, after degradation with an optical model and after noise reconstruction. Comparing the filtered image section in figure 5b with the noisy original image in figure 5c, the space-variant filtering is obvious: In the right part of the image region in figure 5b, the noise still resembles that in figure 5a, while the low-pass effect is clearly noticeable towards the left image edge. After noise reconstruction using our algorithm separately on all three color channels with $W = 9$ and $B = 3$, the noise in the final image, of which the respective section is shown in figure 5c, has the same visual characteristics as the original noise. Comparing the reconstructed image with figure 5b, we note that the effect of the noise reconstruction algorithm is lower in areas where the effect of the filter on the noise is as well, as expected. With regards to the importance of noise reconstruction in the case of high noise levels, we consider figure 6. A section of a driving scene from the BDD100k depicting a person is shown in figure 6a and after corruption with synthetic noise in figure 6b. The PSNR of the noisy image compared to the noise-free image is 25.7dB. After degradation using an optical model, seen in figure 6c, the PSNR is now 25.6dB. Considering the strong low-pass filter effect on the underlying image content, it is not surprising that the PSNR drops slightly despite the lower noise variance detectable by visual inspection. Nonetheless, some remaining correlated noise is visible in figure 6c. After application of the noise reconstruction algorithm to the degraded image, the resulting noise in figure 6d has the desired properties and visually resembles that in figure 6a. The PSNR drops significantly to 22.7dB. Considering the importance of noise reconstruction in the context of computer vision algorithms, this leads to the conclusion that when driving scenes corrupted with noise are used to train such algorithms and the image quality is varied by degradation with optical models, then the noise has to be taken into account. Otherwise, the original camera sensor noise would be neglected to some extent due to low-pass filtering, which could, considering the sensitivity of neural networks often used in computer vision, lead to unexpected results when testing an algorithm on the road.

Impact on CV detection algorithms

The importance of the difference in visual quality of filtered images before and after noise reconstruction is further corroborated by the results presented in Tab. 2, where the average precision results from an object detection algorithm on 21 daytime

(a) Noisy original

(b) Spatially-variant filtering applied to (a)

(c) Noise reconstruction applied to (b)

Figure 5: Demonstrating the space variant behavior of the presented noise reconstruction method

(a) PSNR → (b) 25.7dB (c) 25.6dB (d) 22.7dB

Figure 6: ROI from a driving scene from BDD100k

images from the BDD100k dataset are noted. We assume the original images to be almost noise-free. The drop in average precision after adding noise with parameters $a = 1$ and $b = 50$ is -7% in person detection and -3.9% in car detection. After degradation using a strongly defocused Cooke-Triplet optical model, average precision in these tasks compared to the noise-free unfiltered image drops by -17.2% and -12.2% respectively. Reflecting the influence of noise on the image quality, average precision after application of our method is even lower, at -28.8% for person detection and -21.6% for car detection compared to the precision on ground truth.

	AP person	AP car
ground truth	69.31	81.82
noisy image Δ	-7.3%	-3.9%
degraded	-17.2%	-12.2%
reconstructed	-28.8%	-21.6%

Table 2: Average precision results from 21 daytime images for strongly defocused Cooke-Triplet optical model

Conclusion

In this work, we present an approach to original image noise reconstruction on spatially varying filtered images. To tackle the main challenges of signal-dependent noise and spatially-varying filter characteristics, we combine variance stabilizing transformation with local application of a noise variance estimation method. Our method performs successful image noise parameter reconstruction. Results indicate a drop in average precision of computer vision algorithms after application of our method, demonstrating the importance of noise reconstruction.

For future work, further evaluation of the algorithm on real driving scenes is needed. As no denoising is performed before noise reconstruction, comparison of our method to other possible approaches involving denoising before noise reconstruction might prove useful with regards to the influence on computer vision algorithms. Concerning differences between the original noise distribution and the final reconstructed distribution due to the remaining correlated noise in the latter, which in this work we assume to be negligible due to the relatively low variance of correlated noise but which may change the perceived image content, the use of neural networks such as autoencoders, already applied successfully in image denoising or image generation, may prove an interesting consideration in future work.

References

[1] Abbas Arab, Jamila Harbi, and Amel Abbas. “Image Compression Using Principle Component Analysis”. In: *Al-Mustansiriyah Journal of Science* 29.2 (2018), p. 141.

[2] Uwe Artmann, Marc Geese, and Max Gäde. “Contrast detection probability - Implementation and use cases”. In: *Electronic Imaging* 2019.15 (Jan. 13, 2019), pp. 30–30.

[3] Alexey Kurakin; Ian J. Goodfellow; Samy Bengio. “Adversarial Examples in the Physical World”. In: ed. by Roman V. Yampolskiy. Artificial Intelligence Safety and Security. CRC Press, July 27, 2018. Chap. 8.

[4] Marc Geese, Ulrich Seger, and Alfredo Paolillo. “Detection Probabilities: Performance Prediction for Sensors of Autonomous Vehicles”. In: *Electronic Imaging* 2018.17 (Jan. 28, 2018), pp. 148–1–148–14.

[5] Heiko Hoffmann. “Kernel PCA for novelty detection”. In: *Pattern Recognition* 40.3 (2007), pp. 863–874.

[6] Harold Hotelling. “Analysis of a complex of statistical variables into principal components”. In: *Journal of Educational Psychology* 24.6 (1933), pp. 417–441.

[7] *IEEE Standards Association P2020 — Automotive Image Quality Working Group*. URL: `https://site.ieee.org/sagroups-2020/` (visited on 01/31/2022).

[8] Bernd Jähne. *Digitale Bildverarbeitung*. 5., überarb. und erw. Aufl. Engineering online library. Berlin: Springer, 2002.

[9] Bernd Jähne. *Digitale Bildverarbeitung*. Berlin, Heidelberg: Springer Berlin Heidelberg, 2012.

[10] Robin Jenkin. “Contrast Signal to Noise Ratio”. In: *Electronic Imaging* 2021.17 (Jan. 18, 2021), pp. 186–186.

[11] I. T. Jolliffe. *Principal Component Analysis*. Second Edition. Springer Series in Statistics. New York, NY: Springer-Verlag New York Inc, 2002.

[12] Kasper Winther Jørgensen and Lars Kai Hansen. “Model selection for Gaussian kernel PCA denoising”. In: *IEEE transactions on neural networks and learning systems* 23.1 (2012), pp. 163–168.

[13] Christian Krebs, Patrick Müller, and Alexander Braun. “Impact of Windshield Optical Aberrations on Visual Range Camera Based Classification Tasks Performed by CNNs”. In: *London Imaging Meeting* 2021.1 (Sept. 20, 2021), pp. 83–87.

[14] Matthias Lehmann et al. “Modeling realistic optical aberrations to reuse existing drive scene recordings for autonomous driving validation”. In: *Journal of Electronic Imaging* 28.01 (2019), p. 1.

[15] Matthias Lehmann et al. “Resolution and accuracy of nonlinear regression of point spread function with artificial neural networks”. In: *Optical Engineering* 58.04 (2019), p. 1.

[16] K. V. Mardia. “Measures of Multivariate Skewness and Kurtosis with Applications”. In: *Biometrika* 57.3 (1970), p. 519.

[17] Patrick Mueller, Matthias Lehmann, and Alexander Braun. “Simulating tests to test simulation”. In: *Electronic Imaging*. Vol. 2020. Jan. 26, 2020, pp. 149–1–149–8.

[18] Patrick Müller, Mattis Brummel, and Alexander Braun. “Spatial recall index for machine learning algorithms”. In: *London Imaging Meeting* 2021.1 (Sept. 20, 2021), pp. 58–62.

[19] Patrick Müller, Matthias Lehmann, and Alexander Braun. “Optical quality metrics for image restoration”. In: *Digital Optical Technologies 2019*. Digital Optical Technologies II. Ed. by Bernard C. Kress and Peter Schelkens. Munich, Germany: SPIE, June 21, 2019, p. 37.

[20] Karl Pearson. “LIII. On lines and planes of closest fit to systems of points in space”. In: *The London, Edinburgh, and Dublin Philosophical Magazine and Journal of Science* 2.11 (1901), pp. 559–572.

[21] Zachary Pezzementi et al. “Putting Image Manipulations in Context: Robustness Testing for Safe Perception”. In: *2018 IEEE International Symposium on Safety, Security, and Rescue Robotics (SSRR)*. 2018 IEEE International Symposium on Safety, Security, and Rescue Robotics (SSRR). Philadelphia, PA: IEEE, Aug. 2018, pp. 1–8.

[22] S. Pyatykh, J. Hesser, and Lei Zheng. “Image Noise Level Estimation by Principal Component Analysis”. In: *IEEE Transactions on Image Processing* 22 (2013), pp. 687–699.

[23] Stanislav Pyatykh and Jurgen Hesser. “Image Sensor Noise Parameter Estimation by Variance Stabilization and Normality Assessment”. In: *IEEE transactions on image processing : a publication of the IEEE Signal Processing Society* 23.9 (2014), pp. 3990–3998.

[24] EMVA 1288 Working group. *EMVA Standard 1288 Release 3.1*. Dec. 2016.

[25] Fisher Yu et al. “BDD100K: A Diverse Driving Video Database with Scalable Annotation Tooling”. In: *CoRR* abs/1805.04687 (2018). arXiv: `1805.04687`.

Author Biography

Luis Wohlers is a Master student at Heinrich-Heine Universität Düsseldorf. He received his Bachelor's degree from University of Applied Sciences Düsseldorf in Electrical Engineering and Information Technology.

Patrick Müller received his B.Eng. in 2016 and his M.Sc. in 2018. His Master's thesis examined the influence of a Point Spread Function Model to Digital Image Processing algorithms. He is currently pursuing his PhD with a focus on the application of optical models to digital images, their validation, performance and correlation with the performance of Computer Vision algorithms.

Alexander Braun received his diploma in physics with a focus on laser fluorescent spectroscopy from the University of Göttingen in 2001. His PhD research in quantum optics was carried out at the University of Hamburg, resulting in a Doctorate from the University of Siegen in 2007. He started working as an optical designer for camera-based ADAS with the company Kostal, and became a Professor of Physics at the University of Applied Sciences in Düsseldorf in 2013, where he now researches optical metrology and optical models for simulation in the context of autonomous driving. He's member of DPG, SPIE and IS&T, participating in norming efforts at IEEE (P2020) and VDI (FA 8.13), and currently serves on the advisory board for the AutoSens conference.